molecular pharmaceutics

pubs.acs.org/molecularpharmaceutics

Article

^{68}Ga- and ^{211}At-Labeled RGD Peptides for Radiotheranostics with Multiradionuclides

Kazuma Ogawa,* Hiroaki Echigo, Kenji Mishiro, Saki Hirata, Kohshin Washiyama, Yoji Kitamura, Kazuhiro Takahashi, Kazuhiro Shiba, and Seigo Kinuya

Cite This: https://doi.org/10.1021/acs.molpharmaceut.1c00460

Read Online

ACCESS | Metrics & More | Article Recommendations | Supporting Information

ABSTRACT: Probes for radiotheranostics could be produced by introducing radionuclides with similar chemical characteristics into the same precursors. We recently developed an ^{211}At-labeled RGD peptide and a corresponding radioiodine-labeled RGD peptide. Both labeled peptides accumulated in large quantities in the tumor with similar biodistribution, demonstrating their usefulness for radiotheranostics. In this study, we hypothesized that probes for radiotheranostics combined with multiradionuclides, such as ^{68}Ga and ^{211}At, have useful clinical applications. New radiolabeled RGD peptide probes were synthesized via a molecular design approach, with two labeling sites for metal and halogen. These probes were evaluated in biodistribution experiments using tumor-bearing mice. [^{67}Ga]Ga-DOTA-c[RGDf(4-I)K] ([^{67}Ga]**4**), Ga-DOTA-[^{125}I]c-[RGDf(4-I)K] ([^{125}I]**4**), and Ga-DOTA-[^{211}At]c[RGDf(4-At)K] ([^{211}At]**7**) showed similar biodistribution, with high and equivalent accumulation in tumors. These results indicate the usefulness of these probes in radiotheranostics with multiradionuclides, such as a radiometal and a radiohalogen, and they could contribute to a personalized medicine regimen.

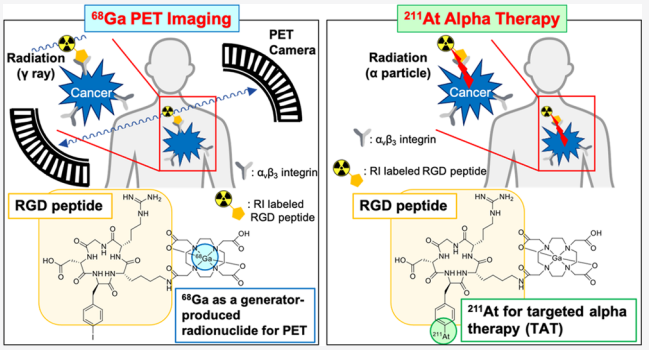

KEYWORDS: *radiotheranostics, astatine-211, RGD peptide, gallium-68, multiradionuclides*

INTRODUCTION

The word "theranostics", a portmanteau of the words "therapeutics" and "diagnostics", means agents or methods that combine diagnostic imaging and targeted therapy.[1] It has recently gathered much attention in oncology.[2] Theranostics with radioisotopes is called "radiotheranostics", and this technique combines imaging in nuclear medicine with positron emission tomography (PET) and single-photon emission computed tomography (SPECT), as well as radionuclide therapy.[3] If a diagnostic probe and a therapeutic probe show the same biodistribution, absorbed doses for the therapeutic probe in the tumor and each normal tissue can be calculated from the quantitative imaging data of PET or SPECT. Namely, therapeutic effects and side effects could become predictable before therapy. Moreover, determining the therapeutic effects at earlier time-points after therapy, before morphological changes in the tumor, should be possible by PET or SPECT imaging. Hence, radiotheranostics can contribute to personalized medicine. Thus, developing diagnostic and therapeutic probes with equivalent biodistribution characteristics is important for a successful radiotheranostics design. In general, the probes for radiotheranostics have been produced by the introduction of elements with similar chemical characteristics into the same precursors.[4,5]

In radionuclide therapy, targeted alpha therapy (TAT) has gained much attention due to the high therapeutic effects derived from the high linear energy transfer (LET) of α-particles.[6,7] For example, a report of excellent therapeutic effects for ^{225}Ac-PSMA to castration-resistant prostate cancer patients was sensational.[8] Thus, actinium-225 (^{225}Ac) is an attractive radionuclide for TAT. However, there has been a shortage in the global supply of ^{225}Ac. Among the α-emitting radionuclides, astatine-211 (^{211}At) has gained considerable attention.[9] The half-life ($t_{1/2}$ = 7.2 h) of ^{211}At is not too short for it to be considered in TAT. ^{211}At decays to ^{207}Bi (42%) with the emission of α-particles (5.9 MeV) and then ^{207}Bi ($t_{1/2}$ = 33.9 years) decays to a stable isotope, ^{207}Pb, via electron capture. ^{211}At also decays to ^{211}Po (58%) via electron capture, with ^{211}Po ($t_{1/2}$ = 516 ms) decaying to ^{207}Pb by emitting α-particles (7.5 MeV).

We recently developed a novel ^{211}At-labeling method using the Arg-Gly-Asp (RGD) peptide as a model peptide.[10] The

Received: June 8, 2021
Revised: August 3, 2021
Accepted: August 4, 2021

^{211}At-labeled RGD peptide, [^{211}At]c[RGDf(4-At)K], and the corresponding radioiodine-labeled RGD peptide, [^{125}I]c-[RGDf(4-I)K], showed high accumulation in the tumor and similar biodistribution, demonstrating their usefulness in a radiotheranostics approach of combining [^{211}At]c[RGDf(4-At)K] with [^{123}I]c[RGDf(4-I)K]. In general, the combination of radionuclides for radiotheranostics has been restricted because only elements with similar chemical characteristics are used, such as halogens or metals, as they can be coordinated with the same ligand. However, if more elements can be combined for radiotheranostics, this would be convenient for clinical applications. For example, we hypothesized that probes with ^{68}Ga, a generator-produced positron emitter for PET imaging, combined with ^{211}At for TAT would be very useful in radiotheranostics.

In this study, we produced probes for multiradionuclide radiotheranostics using a molecular design approach wherein two radiolabeling sites for radiometal and radiohalogen were included. Thus, [^{67}Ga]Ga-DOTA-c[RGDf(4-I)K] ([^{67}Ga]**4**), Ga-DOTA-[^{125}I]c[RGDf(4-I)K] ([^{125}I]**4**), and Ga-DOTA-[^{211}At]c[RGDf(4-At)K] ([^{211}At]**7**) (Figure 1) were designed,

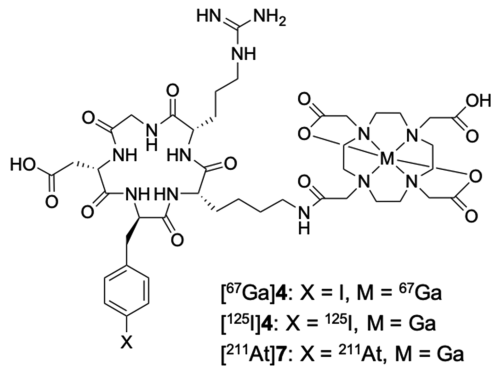

Figure 1. Structures of [^{67}Ga]**4**, [^{125}I]**4**, and [^{211}At]**7**.

synthesized, and evaluated. Although we were interested in ^{68}Ga ($t_{1/2}$ = 68 min) for PET imaging, ^{67}Ga ($t_{1/2}$ = 3.3 days) was used in this basic study as an alternative radionuclide because of its longer half-life.

MATERIALS AND METHODS

Materials. ^{211}At was produced on CYPRIS MP-30 cyclotron (Sumitomo Heavy Industries, Ltd., Tokyo, Japan) in the Advanced Clinical Research Center at Fukushima Medical University via ^{209}Bi(α, 2n)^{211}At nuclear reaction.[11] [^{67}Ga]$GaCl_3$ was supplied by Nihon Medi-Physics Co., Ltd. (Tokyo, Japan). [^{125}I]Sodium iodide (644 GBq/mg) was purchased from PerkinElmer (Waltham, MA). Electrospray ionization mass spectra (ESI-MS) were obtained with a JEOL JMS-T100TD (Jeol Ltd., Tokyo, Japan). Purification and identification of peptides and labeled peptides were performed using an HPLC system (LC-20AD pump, SPD-20A UV detector at a wavelength of 220 nm, and CTO-20A column oven maintained at 40 °C; Shimadzu, Kyoto, Japan). Fmoc-Lys(Boc)-OH was purchased from Merck (Darmstadt, Germany). 2-Chlorotrityl chloride resin, Fmoc-Arg(Pbf)-OH, Fmoc-Asp(O*t*Bu)-OH, Fmoc-Gly-OH, Fmoc-d-Tyr(*t*Bu)-OH, Fmoc-d-Phe-OH, and Fmoc-Val-OH were purchased from Watanabe Chemical Industries, Ltd. (Hiroshima, Japan). 1,4,7,10-Tetraazacyclododecane-1,4,7-tris(*t*-butyl acetate) (DOTA-tris) was purchased from Macrocyclics (Dallas, TX). U-87 MG glioblastoma cells were purchased from DS Pharma Biomedical (Osaka, Japan). Fmoc-4-iodo-D-phenylalanine [Fmoc-D-Phe(4-I)] was synthesized according to a previous report.[12] *N*,*N*-Diisopropylethylamine (DIPEA) was purchased from Nacalai Tesque (Kyoto, Japan). 1,3-Diisopropylcarbodiimide (DIPCDI) and 1-hydroxybenzotriazole hydrate (HOBt) were purchased from Kokusan Chemical Co., Ltd. (Tokyo, Japan). 2-(1*H*-Benzotriazole-1-yl)-1,1,3,3-tetramethylaminium tetrafluoroborate (TBTU) was purchased from Chem Impex International, Inc. (Wood Dale, IL). Other reagents were of reagent grade and used as received.

Synthesis of Reference Compounds and Radiolabeled Compounds. Ga-DOTA-c[RGDf(4-I)K] (**4**) and [^{67}Ga]Ga-DOTA-c[RGDf(4-I)K] ([^{67}Ga]**4**) were synthesized according to the procedure outlined in Scheme 1. DOTA-[^{125}I]c[RGDf(4-I)K] ([^{125}I]**3**), Ga-DOTA-[^{125}I]c[RGDf(4-I)K] ([^{125}I]**4**), and Ga-DOTA-[^{211}At]c[RGDf(4-At)K] ([^{211}At]**7**) were synthesized according to the procedure outlined in Scheme 2.

*Preparation of c[R(Pbf)GD(OtBu)f(4-I)K] (**1**).* Cyclic[Arg-(Pbf)-Gly-Asp(O*t*Bu)-D-Phe(4-I)-Lys] (**1**) was synthesized manually using a standard Fmoc-based solid-phase methodology according to a previous report with slight modifications.[10,13] The crude peptide was purified by reversed-phase (RP)-HPLC on Cosmosil 5C_{18}-AR-II column (20 × 250 mm; Nacalai Tesque) at a flow rate of 12 mL/min with an isocratic mobile phase of 65% methanol in water with 0.1% trifluoroacetic acid (TFA). The fraction containing **1** was determined by mass spectrometry and was collected. The solvent was removed by lyophilization to yield **1** (26.5 mg, 25%) as a white powder.

c[R(Pbf)GD(O*t*Bu)f(4-I)K] (**1**): MS (ESI$^+$) calcd for $C_{44}H_{64}IN_9O_{10}S$ [M + H]$^+$: m/z = 1038.36 found 1038.54.

*Preparation of DOTA(OtBu)$_3$-c[R(Pbf)GD(OtBu)f(4-I)K] (**2**).* DOTA-tris (36.4 mg, 53.0 μmol) was dissolved in 1 mL of dimethylformamide (DMF) and then TBTU (18.5 mg, 48.2 μmol) and DIPEA (19.8 μL, 116 μmol) were added to the solution. After 1 h stirring at room temperature, **1** (10.0 mg, 9.63 μmol) was added to the reaction mixture. After another 1 h stirring, purification was performed by RP-HPLC performed with a Cosmosil 5C_{18}-AR-II column (10 × 250 mm; Nacalai Tesque) at a flow rate of 4 mL/min with a gradient mobile phase of 70% methanol in water with 0.1% TFA to 90% methanol in water with 0.1% TFA for 20 min. The solvent was removed by lyophilization to yield **2** (9.9 mg, 65%) as a white powder.

DOTA(O*t*Bu)$_3$-c[R(Pbf)GD(O*t*Bu)f(4-I)K] (**2**): MS (ESI$^+$) calcd for $C_{72}H_{114}IN_{13}O_{17}S$ [M + H]$^+$: m/z = 1592.73, found 1593.49.

*Preparation of DOTA-c[RGDf(4-I)K] (**3**).* Compound **2** (10.0 mg, 6.28 μmol) was treated with a mixture of 95% TFA, 2.5% water, and 2.5% triisopropylsilane (TIS) for 2 h at room temperature. The crude peptide was purified by RP-HPLC on Cosmosil 5C_{18}-AR-II column (10 × 250 mm) at a flow rate of 4 mL/min with a gradient mobile phase of 30% methanol in water with 0.1% TFA to 50% methanol in water with 0.1% TFA for 20 min. The solvent was removed by lyophilization to yield **3** (5.9 mg, 84%) as a white powder.

DOTA-c[RGDf(4-I)K] (**3**): MS (ESI$^+$) calcd for $C_{43}H_{66}IN_{13}O_{14}$ [M + H]$^+$: m/z = 1116.40, found 1116.01.

*Preparation of Ga-DOTA-c[RGDf(4-I)K] (**4**).* Ga complexation was performed according to a previous report with slight

https://doi.org/10.1021/acs.molpharmaceut.1c00460
Mol. Pharmaceutics XXXX, XXX, XXX−XXX

Scheme 1. Synthetic Scheme of 4 and [^{67}Ga]4[a]

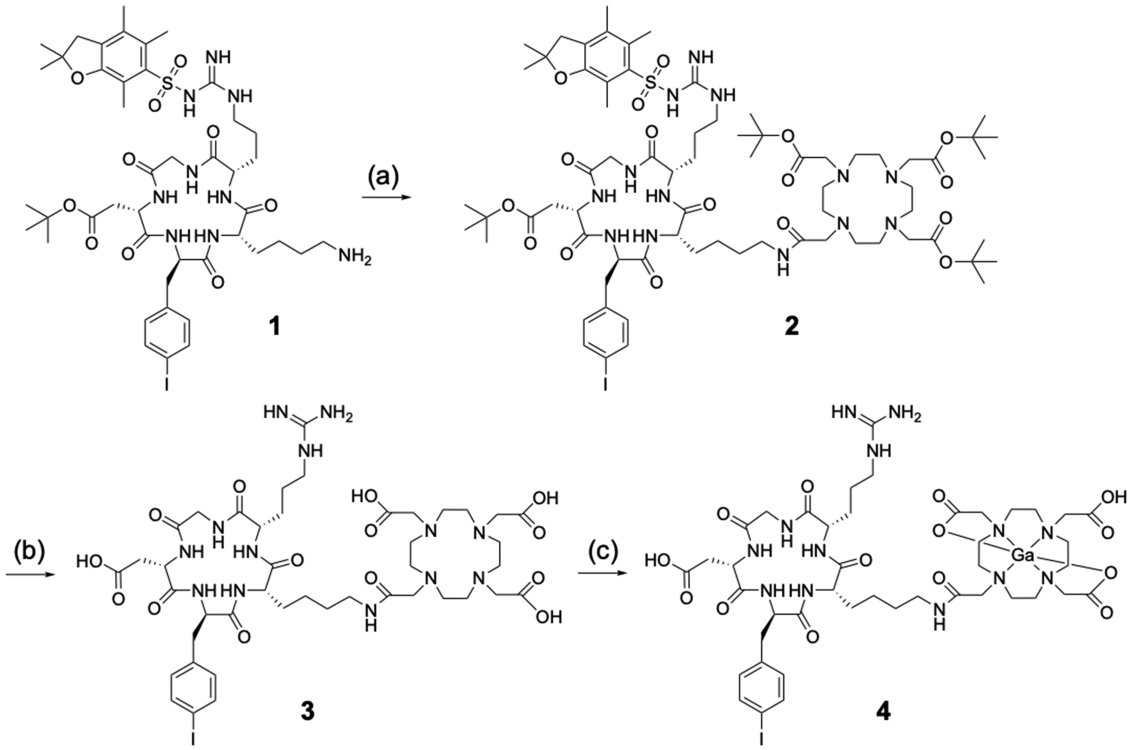

[a]Reagents: (a) DOTA-tris, TBTU, DIPEA, DMF; (b) TFA, water, TIS; (c) $Ga(NO_3)_3$ or [^{67}Ga]$GaCl_3$, ammonium acetate buffer.

Scheme 2. Synthetic Scheme of [^{125}I]4 and [^{211}At]7[a]

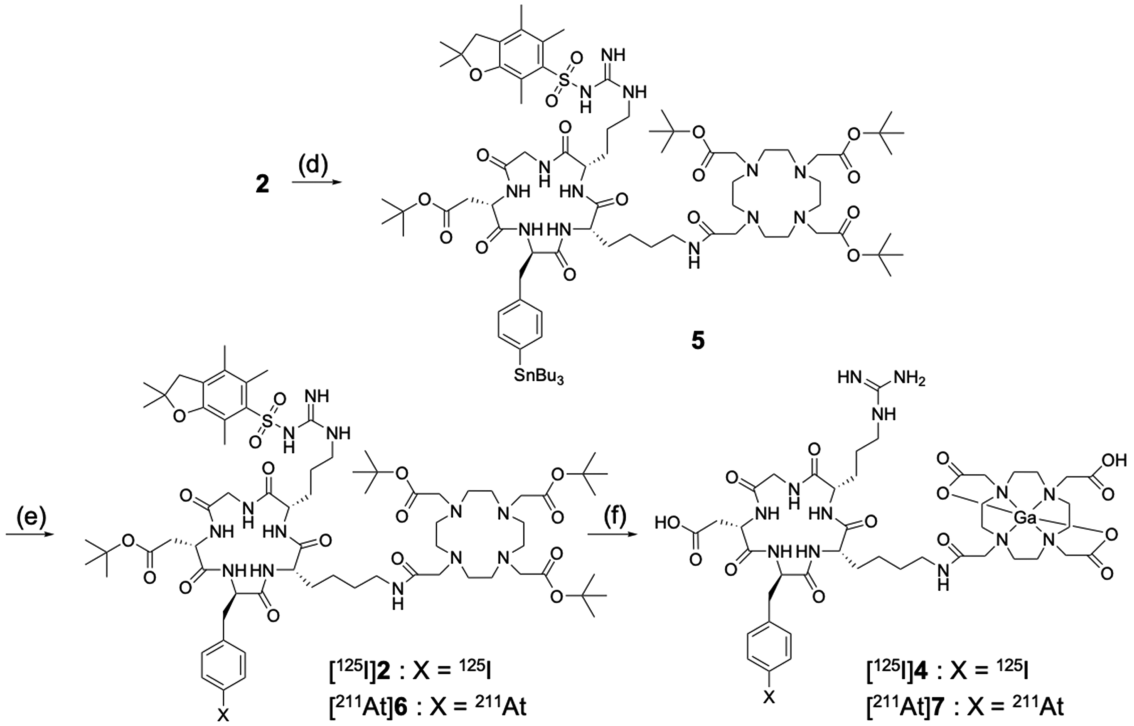

[a]Reagents: (d) Bis(tributyltin), tris(dibenzylideneacetone)dipalladium(0), DIPEA, methanol; (e) [^{125}I]NaI or [^{211}At]At^-, NCS, acetic acid, acetonitrile; (f) (i) TFA, water, TIS and (ii) $Ga(NO_3)_3$, ammonium acetate buffer.

modifications.[14] Compound **3** (1.0 mg, 896 nmol) was dissolved in 500 μL of 1 M ammonium acetate buffer (pH 5.0), and $Ga(NO_3)_3$ (2.29 mg, 8.96 μmol) was added to the solution. The mixture was stirred at 40 °C for 5 min and purified by RP-HPLC performed with Cosmosil 5C_{18}-AR-II (10 × 250 mm) at a flow rate of 4 mL/min with a gradient mobile phase of 30% methanol in water with 0.1% TFA to 50% methanol in water with 0.1% TFA for 20 min. The solvent was

https://doi.org/10.1021/acs.molpharmaceut.1c00460
Mol. Pharmaceutics XXXX, XXX, XXX−XXX

removed by lyophilization to yield **4** (332 μg, 29%) as a white powder.

Ga-DOTA-c[RGDf(4-I)K] (**4**): MS (ESI$^+$) calcd for $C_{43}H_{64}GaIN_{13}O_{14}$ $[M + 2H]^{2+}$: m/z = 592.16, found 591.43.

*Preparation of [^{67}Ga]Ga-DOTA-c[RGDf(4-I)K] ([^{67}Ga]**4**).* Compound **3** (50 μg) was dissolved in 30 μL of 1 M ammonium acetate buffer, pH 5.0, and 30 μL of [^{67}Ga]$GaCl_3$ (1.6 MBq) was added to the solution. The mixture was reacted at 80 °C for 5 min. [^{67}Ga]**4** was purified by RP-HPLC performed with Cosmosil 5C_{18}-AR-II (4.6 × 150 mm) at a flow rate of 1 mL/min with an isocratic mobile phase of 30% methanol in water with 0.1% TFA. The radiochemical yield of [^{67}Ga]**4** was 97%. The radiochemical purity of [^{67}Ga]**4** was >99%.

*DOTA(OtBu)$_3$-c[R(Pbf)GD(OtBu)f[4-Sn(nBu)$_3$]K] (**5**).* Compound **2** (500 μg, 628 nmol) was dissolved in 500 μL of methanol. Bis(tributyltin) (1.27 μL, 2.51 μmol), tris-(dibenzylideneacetone)dipalladium(0) (86.2 μg, 94.1 nmol), and DIPEA (0.26 μL, 1.57 μmol) were added to the solution of **2**. After stirring at 60 °C for 1 h, the reaction mixture was purified by RP-HPLC with a Cosmosil 5C_{18}-AR-II column (10 × 150 mm) at a flow rate of 4 mL/min with a gradient mobile phase of 80% methanol in water with 0.1% TFA to 100% methanol with 0.1% TFA for 20 min. The solvent was removed by lyophilization to yield **5**.

DOTA(O*t*Bu)$_3$-c[R(Pbf)GD(O*t*Bu)f[4-Sn(*n*Bu)$_3$]K] (**5**) MS (ESI$^+$) calcd for $C_{84}H_{141}N_{13}O_{17}SSn$ $[M + 2H]^{2+}$: m/z = 878.97, found 878.71.

*Preparation of DOTA-[^{125}I]c[RGDf(4-I)K] ([^{125}I]**3**).* A small amount of **5** was dissolved in 5 μL of acetonitrile in the reaction vial. Ten microliters of 1% acetic acid in acetonitrile, 3 μL of [^{125}I]NaI (3.7 MBq) solution, and 15 μL of *N*-chlorosuccinimide (NCS) in acetonitrile (1 mg/mL) were added to the vial. After heating at 80 °C for 15 min, the reaction mixture was quenched with 15 μL of $NaHSO_3$ solution (1 mg/mL). After evaporating the solvent using N_2 gas, the residue was treated in 100 μL of a mixture of 95% TFA, 2.5% water, and 2.5% TIS for 90 min at room temperature and then purified by RP-HPLC with a Cosmosil 5C_{18}-AR-II column (4.6 × 150 mm) at a flow rate of 1 mL/min with a gradient mobile phase of 30% methanol in water with 0.1% TFA to 50% methanol in water with 0.1% TFA for 20 min. The radiochemical yield of [^{125}I]**3** was 29%. The radiochemical purity of [^{125}I]**3** was >97%.

*Preparation of Ga-DOTA-[^{125}I]c[RGDf(4-I)K] ([^{125}I]**4**).* Ten microliters of [^{125}I]**3** was mixed with 90 μL of $Ga(NO_3)_3$ (1 mg/mL) in 1 M ammonium acetate buffer (pH 5.0). After standing at 40 °C for 5 min, [^{125}I]**4** was purified by RP-HPLC performed with Cosmosil 5C_{18}-AR-II (4.6 × 150 mm) at a flow rate of 1 mL/min with an isocratic mobile phase of 30% methanol in water with 0.1% TFA. The radiochemical yield of [^{125}I]**4** was 84%. The radiochemical purity of [^{125}I]**4** was >96%.

*Preparation of Ga-DOTA-[^{211}At]c[RGDf(4-At)K] ([^{211}At]**7**).* A small amount of **5** was dissolved in 5 μL of acetonitrile in the reaction vial. Ten microliters of 1% acetic acid in acetonitrile, 3 μL of the [^{211}At]At^- solution, and 15 μL of *N*-chlorosuccinimide (NCS) in acetonitrile (1 mg/mL) were added to the vial. After heating for 15 min at 80 °C, the reaction mixture was quenched with 15 μL of $NaHSO_3$ solution (1 mg/mL). After evaporating the solvent using N_2 gas, the residue was treated in 100 μL of a mixture of 95% TFA, 2.5% water, and 2.5% TIS for 60 min at room temperature, and then purified by RP-HPLC with a Cosmosil 5C_{18}-AR-II column (4.6 × 150 mm) at a flow rate of 1 mL/min with a gradient mobile phase of 30% methanol in water with 0.1% TFA to 50% methanol in water with 0.1% TFA for 20 min. The radiochemical yield of DOTA-[^{211}At]c[RGDf(4-At)K] ([^{211}At]**6**) was 16%. The radiochemical purity of [^{211}At]**6** was >97%.

Ten microliters of [^{211}At]**6** was mixed with 90 μL of $Ga(NO_3)_3$ (1 mg/mL) in 1 M ammonium acetate buffer, pH 5.0. After standing at 40 °C for 5 min, [^{211}At]**7** was purified by RP-HPLC performed with Cosmosil 5C_{18}-AR-II (4.6 × 150 mm) at a flow rate of 1 mL/min with an isocratic mobile phase of 30% methanol in water with 0.1% TFA. The radiochemical yield of [^{211}At]**7** was 36%. The radiochemical purity of [^{211}At]**7** was >96%.

$\alpha_v\beta_3$ Integrin-Binding Assay. Binding affinities of synthesized peptides, c(RGDfK), c[RGDf(4-I)K], **3**, and **4**, for $\alpha_v\beta_3$ integrin were evaluated by competitive inhibition between the peptides and [^{125}I]c[RGDy(3-I)V], which was prepared by Fmoc solid-phase synthesis and following the chloramine-T method,[15] according to a previously reported procedure.[16] The half-maximal inhibitory concentration (IC_{50}) values of the peptides were calculated by curve fitting with nonlinear regression using GraphPad Prism 5.04 (GraphPad Software Inc., San Diego, CA). Each data point is the average of four determinations, and IC_{50} values were expressed as mean ± standard deviation (SD) from three independent experiments.

***In Vitro* Stability.** To evaluate the stability of [^{67}Ga]**4**, [^{125}I]**4**, and [^{211}At]**7** in PBS(−), 10 μL of each tracer (37 kBq) was added to 80 μL of PBS(−) (pH 7.4) and the solutions were incubated at 37 °C for 1 for [^{211}At]**7** or 24 h for [^{67}Ga]**4** and [^{125}I]**4**. After 1 and 24 h incubation, the samples were drawn, and the radioactivity was analyzed by RP-HPLC.

***In Vitro* Cellular Uptake.** Cellular uptake experiments were performed according to a previous report with a slight modification.[17] U-87 MG was cultured in Eagle's minimum essential medium (EMEM) containing 10% fetal bovine serum (FBS) on six-well culture plates (containing 1 × 10^6 cells/well) for 24 h using a humidified atmosphere (5% CO_2) incubator at 37 °C. After the removal of the medium, a mixed solution of [^{67}Ga]**4** and [^{125}I]**3**, [^{67}Ga]**4**, and [^{125}I]**4** or [^{125}I]**4** and [^{211}At]**7** (3.7 kBq/each tracer/well) in the medium without FBS was added. After incubation for 1, 3, and 6 h, the medium from each well was removed and the cells were washed twice with an ice-cold EMEM. The surface of the cells was washed twice with an ice-cold 0.2 M glycine buffer, pH 3.0. The cells were lysed using a 1 M NaOH aqueous solution. The radioactivity in glycine buffer and 1 M NaOH was determined using an auto-well γ-counter. The radioactivity in glycine buffer and 1 M NaOH was defined as membrane-bound radioligand fraction (MRF) and internalized radioligand fraction (IRF), respectively. Internalized rate was defined by the following formula.

$$\text{internalized rate}(\%) = \text{IRF}/(\text{MRF} + \text{IRF})$$

The protein amount of cells was quantified using a BCA protein assay kit (Nacalai Tesque) according to the manufacturer's protocol. All data were expressed as percent dose per milligram protein (%dose/mg protein).

In blocking experiments, c(RGDfK) (final concentration of 10 μM) was added to each well with tracers. After incubation for 6 h, radioactivity and protein concentration were determined using the same method mentioned above.

https://doi.org/10.1021/acs.molpharmaceut.1c00460
Mol. Pharmaceutics XXXX, XXX, XXX−XXX

Biodistribution of [^{67}Ga]Ga-DOTA-c[RGDf(4-At)K] ([^{67}Ga]4), DOTA-[^{125}I]c[RGDf(4-I)K] ([^{125}I]3), Ga-DOTA-[^{125}I]c[RGDf(4-I)K] ([^{125}I]4), and Ga-DOTA-[^{211}At]c[RGDf-(4-At)K] ([^{211}At]7) in Tumor-Bearing Mice. Experiments with animals were conducted in strict accordance with the Guidelines for the Care and Use of Laboratory Animals of Kanazawa University. The experimental protocols were approved by the Committee on Animal Experimentation of Kanazawa University. The animals were housed with free access to food and water at 23 °C with a 12 h alternating light/dark schedule. U-87 MG cells were grown and injected subcutaneously into 4-week-old female BALB/c nude mice (15−19 g, Japan SLC, Inc., Hamamatsu, Japan) as previously reported.[13] Biodistribution experiments were performed approximately 14 days postinoculation. A mixed solution of [^{67}Ga]**4** (37 kBq) and [^{125}I]**3** (37 kBq), [^{67}Ga]**4** (37 kBq) and [^{125}I]**4** (37 kBq), or [^{125}I]**4** (37 kBq) and [^{211}At]**7** (37 kBq) was intravenously administered to groups of four mice. The mice were sacrificed 1, 4, and 24 h postinjection in the case of the mixture of [^{67}Ga]**4** and [^{125}I]**4** and 1 h postinjection in the cases of the mixture of [^{67}Ga]**4** and [^{125}I]**3** and the mixture of [^{125}I]**4** and [^{211}At]**7**. To determine the amount and routes of the radioactivity excreted from the body for 24 h after injection of [^{67}Ga]**4** and [^{125}I]**4**, the mice were housed in metabolic cages (Metabolica, Sugiyama-Gen Co., Ltd., Tokyo, Japan).

Tissues of interest were removed and weighed. A neck containing thyroid was resected. The thyroid weight to body weight ratio of mice was assumed to be 0.093 mg/g.[18] Radioactivity in the thyroid was calculated assuming that the neck other than the thyroid gland is muscle. The radioactivity counts of ^{67}Ga,^{125}I, and ^{211}At were determined with an auto-well γ-counter (ARC-7010 or ARC-8001, Hitachi, Ltd., Tokyo, Japan) and corrected for background radiation and physical decay during counting. A window from 70 to 400 keV was used for counting ^{67}Ga, a window from 16 to 69 keV was used for counting ^{125}I, and a window from 70 to 120 keV was used for counting ^{211}At. Correlation factors to eliminate any crossover of ^{125}I activity in the ^{67}Ga or ^{211}At counts were determined by measuring the ^{125}I standard in each window. More than one month or one week after the experiments, the radioactivity counts of ^{125}I were measured after attenuation of ^{67}Ga or ^{211}At, respectively.

To investigate the effect of an excess amount of RGD peptide on biodistribution, the U-87 MG tumor-bearing mice were intravenously administered 100 μL of a mixed solution of [^{67}Ga]**4** (37 kBq), [^{125}I]**4** (37 kBq), and c(RGDfK) peptide (0.2 mg/mouse). Mice (n = 4) were sacrificed at 1 h postinjection, and biodistribution experiments were conducted as described above.

SPECT/CT Imaging and Data Reconstruction. SPECT/CT imaging of [^{67}Ga]**4** in the above-mentioned tumor-bearing mice was performed using a small animal SPECT system (VECTor/CT, MIlabs, Houten, The Netherlands). SPECT scanning was performed for 2 h from 4 h postinjection of [^{67}Ga]**4** (10 MBq). The mice were sacrificed at 4 h postinjection because of the long acquisition time of SPECT scanning.

Data were acquired in list mode and photopeak windows were set after the acquisition. The energy windows of 80−110, 165−200, 265−320, and 350−410 keV were employed. Data were reconstructed using pixel-based order subset expectation maximization, with correction for attenuation on computed tomography, in 16 subsets and 6 iterations. The voxel size was 0.8 × 0.8 × 0.8 mm. The obtained SPECT/CT images were analyzed using an image-processing application (AMIDE Imaging software, version 1.0.4).

Statistical Evaluation. Double-tracer experiments were compared using paired Student's t test. Blocking studies were compared using unpaired Student's t test. Differences of IC_{50} values in $\alpha_v\beta_3$ integrin-binding assay were analyzed by one-way analysis of variance (ANOVA). The level of statistical significance was set to $p < 0.05$.

RESULTS AND DISCUSSION

Preparation of [^{67}Ga]4, [^{125}I]4, and [^{211}At]7. Scheme 1 depicts that after **1** was synthesized by the Fmoc solid-phase synthesis, **2** was synthesized by conjugation of DOTA-tris with **1**. To prepare [^{67}Ga]**4**, after deprotection of protection groups of **2**, ^{67}Ga-labeling was performed with a high radiochemical yield (97%) and purity (99%). The iodine molecule in **2** was replaced by a tributylstannyl group via a Pd-catalyzed stannylation reaction to synthesize [^{125}I]**4** and [^{211}At]**7** (Scheme 2). Then, we performed ^{125}I- and ^{211}At-labeling, deprotection of the protecting groups, and Ga complexation. The radiochemical yields of [^{125}I]**4** and [^{211}At]**7** were 25 and 6%, respectively. After HPLC purification, [^{125}I]**4** and [^{211}At]**7** had radiochemical purities of over 96%. Although [^{67}Ga]**4** was prepared in high radiochemical yields in a short labeling time, the radiochemical yields of [^{125}I]**4** and [^{211}At]**7** were low and the radiolabeling procedure was of three steps and complicated. The deprotection of protecting groups of DOTA after the ^{125}I- and ^{211}At-labeling reactions was performed because the Pd-catalyzed stannylation reaction failed after deprotection. A modification of the labeling method might be necessary to improve the radiochemical yields of [^{125}I]**4** and [^{211}At]**7**.

Determination of Radiolabeled Compounds Using HPLC Analyses. The identities of [^{67}Ga]**4** and [^{125}I]**4** were verified by comparing their retention times with that of **4** (Figure 2). However, there are no stable isotopes for astatine. The corresponding nonradioactive compounds cannot be produced to determine the structures for ^{211}At-labeled compounds. Therefore, a nonradioactive iodine element is generally used instead of astatine to determine the structures of

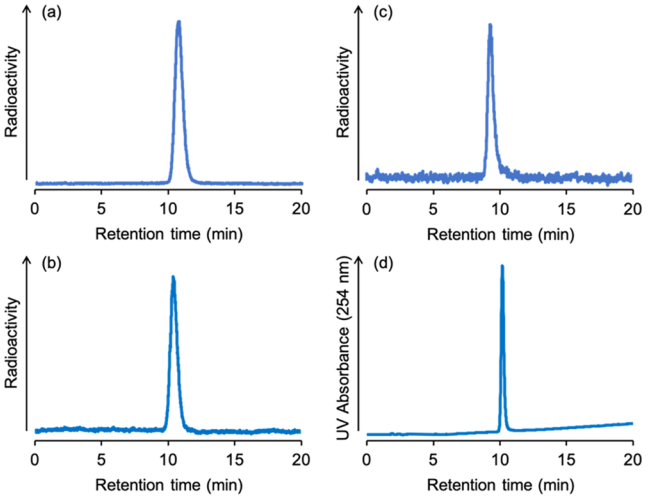

Figure 2. RP-HPLC chromatograms of (a) [^{67}Ga]**4**, (b) [^{125}I]**4**, (c) [^{211}At]**7**, and (d) **4**. Conditions: flow rate was 1 mL/min with an isocratic mobile phase of 30% methanol in water with 0.1% TFA.

https://doi.org/10.1021/acs.molpharmaceut.1c00460
Mol. Pharmaceutics XXXX, XXX, XXX−XXX

^{211}At-labeled compounds,[19] similar to a relationship between technetium and rhenium.[20] Thus, the identity of [^{211}At]**7** was verified by comparing its retention time with that of **4** (Figure 2).

***$\alpha_v\beta_3$* Integrin-Binding Assay.** The affinity of c(RGDfK), c[RGDf(4-I)K], **3**, and **4** for $\alpha_v\beta_3$ integrin was determined via a competitive binding assay using U-87 MG cells. Representative results of the assay are shown in Figure 3. Binding of

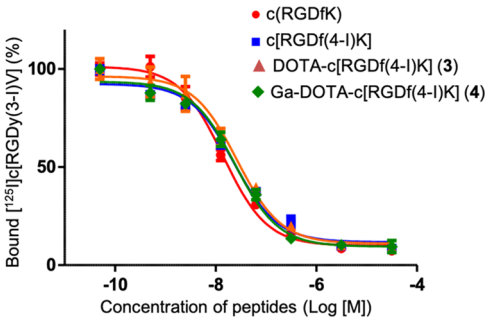

Figure 3. Integrin-binding assay. Representative displacement curves of the competitive binding to $\alpha_v\beta_3$ integrin expressed U-87 MG cells of [^{125}I]c[RGDy(3-I)V] with c(RGDfK), c[RGDf(4-I)K], **3**, and **4**. Error bars represent SD.

[^{125}I]c[RGDy(3-I)V] to $\alpha_v\beta_3$ suffered competition by c(RGDfK), c[RGDf(4-I)K], **3**, and **4** in a concentration-dependent manner. The IC_{50} values (nM) for c(RGDfK), c[RGDf(4-I)K], **3**, and **4** were 10.9 ± 4.2, 23.2 ± 17.2, 30.3 ± 3.4, and 29.9 ± 5.2, respectively. These values were not significantly different. Therefore, the introduction of an iodine molecule into the phenylalanine residue and additionally a DOTA chelator or a Ga-DOTA complex into the ε-amino group of the lysine residue did not significantly impede the affinity of c(RGDfK) for $\alpha_v\beta_3$ integrin. These results are consistent with previous reports showing that the affinities of c(RGDfK) and DOTA-c(RGDfK) for $\alpha_v\beta_3$ integrin were equivalent.[21]

***In Vitro* Stability.** *In vitro* stability experiments of [^{67}Ga]**4**, [^{125}I]**4**, and [^{211}At]**7** were performed in PBS(−) (pH 7.4). After incubation of [^{211}At]**7** for 1 h and [^{67}Ga]**4** and [^{125}I]**4** for 24 h at 37 °C, the radiochemical purities of [^{67}Ga]**4**, [^{125}I]**4**, and [^{211}At]**7** were 95.2 ± 1.2, 95.6 ± 0.4, and 95.2 ± 0.2% (mean ± SD for three samples), respectively. The results indicate that [^{67}Ga]**4**, [^{125}I]**4**, and [^{211}At]**7** were stable in PBS(−).

***In Vitro* Cellular Uptake.** Figure 4 shows the cellular uptake results of [^{67}Ga]**4** and [^{125}I]**3**, [^{67}Ga]**4** and [^{125}I]**4**, or [^{125}I]**4** and [^{211}At]**7** toward U-87 MG cells at 1, 3, and 6 h. The uptake of [^{67}Ga]**4** and [^{125}I]**4** in U-87 MG cells showed almost no difference. The uptake of [^{125}I]**4** and [^{211}At]**7** was also similar. These results indicate that the substitution of astatine for iodine does not alter the tracer's cellular uptake. In contrast, the uptake of [^{125}I]**3**, wherein Ga is not coordinated with DOTA, was lower than that of [^{67}Ga]**4**. Compounds **3** and **4** showed the same degree of affinity for $\alpha_v\beta_3$ integrin. Therefore, the results of the cellular uptake study are inconsistent with the results of the $\alpha_v\beta_3$ integrin-binding assay, although the cause is unclear. Figure 5 shows the internalized rates of [^{67}Ga]**4**, [^{125}I]**3**, [^{125}I]**4**, and [^{211}At]**7** into U-87 MG cells in the cellular uptake study. The internalized rates were similar among tracers and tended to increase in a time-dependent manner.

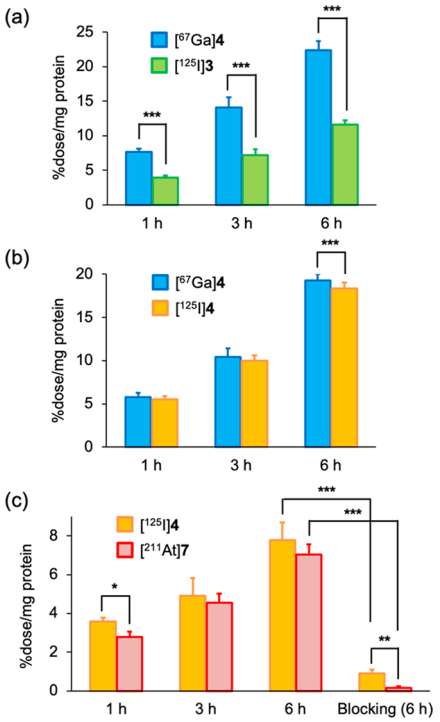

Figure 4. Cellular uptake study. Time-dependent accumulation of (a) [^{67}Ga]**4** and [^{125}I]**3**, (b) [^{67}Ga]**4** and [^{125}I]**4**, and (c) [^{125}I]**4** and [^{211}At]**7** in U-87 MG cells. *In vitro* blocking studies for 6 h incubation of (c) [^{125}I]**4** and [^{211}At]**7** in U-87 MG cells. Data were presented as mean ± SD for three samples. *p < 0.05, **p < 0.01, ***p < 0.001.

Uptakes of [^{125}I]**4** and [^{211}At]**7** in U-87 MG cells were significantly reduced by adding excess amounts of the c(RGDfK) peptide in *in vitro* blocking studies, suggesting that the uptake of [^{125}I]**4** and [^{211}At]**7** is caused by specific binding to $\alpha_v\beta_3$ integrin (Figure 4).

Animal Experiments. In this study, [^{67}Ga]**4** and [^{125}I]**3**, [^{67}Ga]**4** and [^{125}I]**4**, or [^{125}I]**4** and [^{211}At]**7** were co-injected into tumor-bearing mice. The double-tracer experiments can minimize the number of mice and experimental errors. Results of the biodistribution experiments of [^{67}Ga]**4** and [^{125}I]**3**, [^{67}Ga]**4** and [^{125}I]**4**, and [^{125}I]**4** and [^{211}At]**7** in U-87 MG tumor-bearing mice are shown in Figures 6−8 (Tables S1−S3), respectively. Their biodistribution patterns were very similar, such as high tumor uptake and low uptake in other nontarget tissues, except the kidneys and liver as well as the intestine for excretion. Radioactivity in urine and feces at 24 h postinjection of [^{67}Ga]**4** and [^{125}I]**4** showed that the main excretion route of them is urinary excretion; meanwhile, some radioactivity was excreted from the intestine into feces (Table S2). There is no extremely high radioactivity in any tissues in biodistribution data at 1 h postinjection. Therefore, we suppose that much radioactivity had been transferred to the urinary bladder via kidneys before 1 h.

However, regarding the comparison of [^{67}Ga]**4** and [^{125}I]**3**, tumor accumulation of [^{125}I]**3** was significantly lower than that of [^{67}Ga]**4**; this is in accordance with the result of the *in vitro* cellular uptake study. These results indicate that coordination of gallium with DOTA is required for a higher accumulation of this tracer in the tumor. Although lipophilicities of **3** and **4** should be similar, due to their similar retention times in HPLC, their charges must be different depending on the coordination of gallium. Therefore, it is possible that the

https://doi.org/10.1021/acs.molpharmaceut.1c00460
Mol. Pharmaceutics XXXX, XXX, XXX−XXX

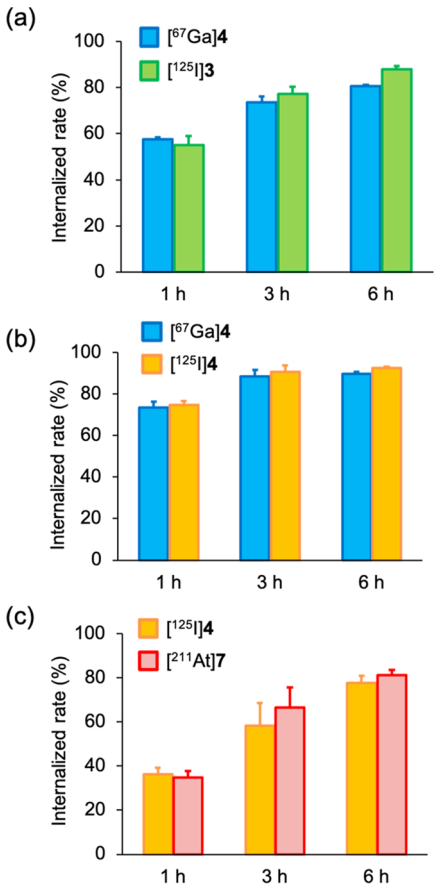

Figure 5. Rates of internalization. Time-dependent rates of internalization in cellular uptake study. Internalized rates of (a) [^{67}Ga]**4** and [^{125}I]**3**, (b) [^{67}Ga]**4** and [^{125}I]**4**, and (c) [^{125}I]**4** and [^{211}At]**7** were expressed as the percentage of the internalized radioactivity in the internalized and membrane-bound radioactivity. Data were presented as mean ± SD for three samples.

negative charges of DOTA may affect tumor accumulation for the RGD peptide. Moreover, the difference in the charges might affect the whole biodistribution because the biodistribution patterns of [^{67}Ga]**4** and [^{125}I]**3** were a little different compared with those of [^{67}Ga]**4** and [^{125}I]**4**.

Regarding [^{67}Ga]**4** and [^{125}I]**4**, the biodistributions of both labeled compounds were almost the same, especially at 1 h. In the concept of radiotheranostics, forming stable radiolabeled compounds is very important for them to have equivalent biodistribution. The equivalent biodistribution of [^{67}Ga]**4** and [^{125}I]**4** indicates that both tracers were hardly decomposed and metabolized *in vivo*, especially until 1 h postinjection. As it is known that free iodine accumulates in the stomach and thyroid, and that free gallium shows delayed blood clearance and high bone accumulation,[22] the low accumulation of [^{67}Ga]**4** and [^{125}I]**4** in those tissues means that deiodination and decomposition of the gallium complex barely occurred. At 24 h postinjection, the biodistribution of [^{67}Ga]**4** and [^{125}I]**4** was slightly different. It may be caused by different radioactive metabolites derived from [^{67}Ga]**4** and [^{125}I]**4**.

In general, *in vivo* stability of the ^{211}At-labeled compound is lower than that of radioiodine-labeled compounds.[23,24] Deastatination in ^{211}At-labeled compounds derived from their *in vivo* lower stability is sometimes a problem for TAT with ^{211}At.[11,25] Nevertheless, the similar biodistribution of [^{125}I]**4** and [^{211}At]**7** in this study indicates that [^{211}At]**7** was stable not only *in vitro* but also *in vivo*. As it is known that free astatine accumulates in the stomach like iodine,[26] the low accumulation of [^{211}At]**7** in the stomach means that deastatination was negligible.

A *in vivo* blocking study was performed to evaluate whether tumor accumulation occurred specifically via $\alpha_v\beta_3$ integrin. Tumor accumulation of [^{67}Ga]**4** and [^{125}I]**4** at 1 h after injection decreased dramatically by co-injection with an excess of c(RGDfK) (0.2 mg/mouse) (Figure 9, Table S2). These results are consistent with the tumor accumulation of [^{67}Ga]**4** and [^{125}I]**4** being caused by their specific binding via $\alpha_v\beta_3$ integrin. In contrast, accumulation of [^{67}Ga]**4** and [^{125}I]**4** in other normal tissues, such as liver and spleen, significantly decreased. Similar results, namely, decreased accumulation in normal tissues in the blocking study, have been reported in previous studies.[27,28] It is known that $\alpha_v\beta_3$ integrin is expressed in microvessels of normal tissues, such as liver and lung.[29] Thus, the results of the blocking study confirm that [^{67}Ga]**4** and [^{125}I]**4** are reasonable as $\alpha_v\beta_3$ integrin-directed peptides.

SPECT/CT Imaging. SPECT/CT images are displayed in Figure 10. The time point of SPECT imaging was set at 4 h postinjection of [^{67}Ga]**4**. As the application as a ^{68}Ga-PET tracer is expected, delayed scanning later than 4 h should be meaningless due to the short half-life of ^{68}Ga. The SPECT images showed a high accumulation of radioactivity in the

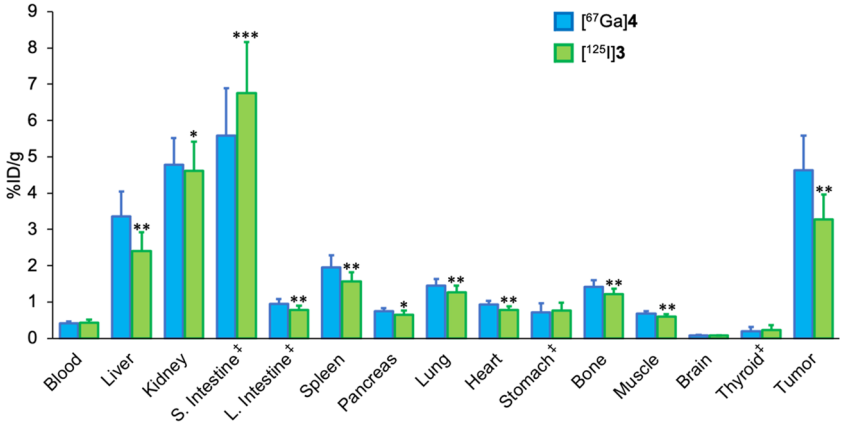

Figure 6. Biodistribution experiments. Biodistribution of radioactivity at 1 h after concomitant intravenous injection of [^{67}Ga]**4** and [^{125}I]**3** in U-87 MG tumor-bearing mice. ‡Expressed as % injected dose. *$p < 0.05$, **$p < 0.01$, ***$p < 0.001$ vs [^{67}Ga]**4**.

https://doi.org/10.1021/acs.molpharmaceut.1c00460
Mol. Pharmaceutics XXXX, XXX, XXX−XXX

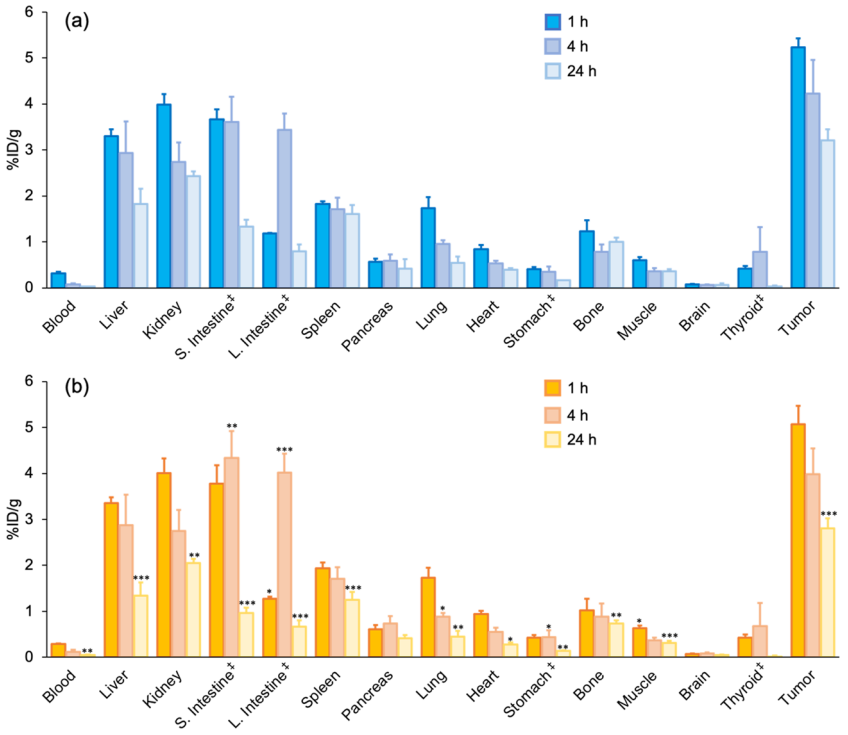

Figure 7. Biodistribution experiments. Biodistribution of radioactivity at 1, 4, and 24 h after concomitant intravenous injection of (a) [^{67}Ga]**4** and (b) [^{125}I]**4** in U-87 MG tumor-bearing mice. ‡Expressed as % injected dose. *p < 0.05, **p < 0.01, ***p < 0.001 vs [^{67}Ga]**4**.

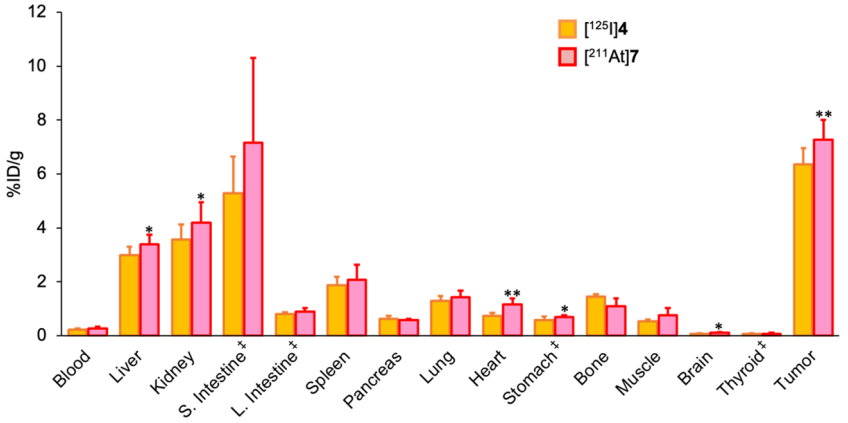

Figure 8. Biodistribution experiments. Biodistribution of radioactivity at 1 h after concomitant intravenous injection of [^{125}I]**4** and [^{211}At]**7** in U-87 MG tumor-bearing mice. ‡Expressed as % injected dose. *p < 0.05, **p < 0.01 vs [^{125}I]**4**.

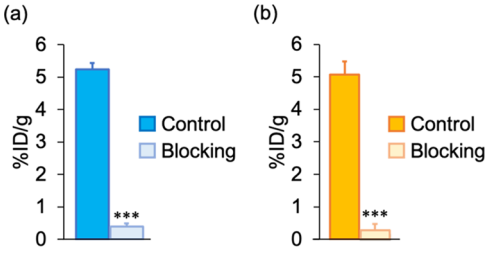

Figure 9. Blocking study. Comparison of tumor uptake of (a) [^{67}Ga]**4** and (b) [^{125}I]**4** at 1 h postinjection under no-carrier-added conditions and with co-injection of an excess of c(RGDfK). ***p < 0.001 vs control.

tumor at 4 h postinjection of [^{67}Ga]**4**. Although the accumulation of radioactivity in the abdominal organs, probably intestine, liver, and kidneys, was a little high, that in the other tissues was lower. These are consistent with the results of the biodistribution experiments.

CONCLUSIONS

In this study, we developed probes for radiotheranostics with ^{68}Ga, which is a generator-produced positron emitter, and ^{211}At for TAT. A similar biodistribution pattern among [^{67}Ga]**4**, [^{125}I]**4**, and [^{211}At]**7** indicates that radiotheranostics in which ^{68}Ga is combined with ^{211}At should be applied using a molecular design with two labeling sites for metal and halogen. By applying this concept, radiotheranostics using multi-radionuclides might be feasible, opening up possibilities to combine other radiohalogens, such as ^{18}F and ^{76}Br as positron emitters for PET, with other radiometals, such as ^{90}Y, ^{177}Lu, $^{212/213}$Bi, and ^{225}Ac as therapeutic radionuclides, which can form a stable complex with some ligand. For radiotheranostics,

https://doi.org/10.1021/acs.molpharmaceut.1c00460
Mol. Pharmaceutics XXXX, XXX, XXX−XXX

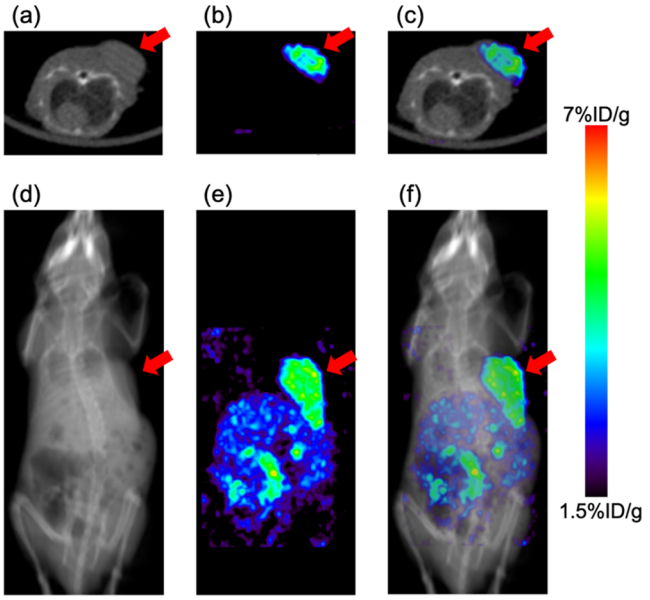

Figure 10. Representative SPECT/CT images. (a) Axial CT image, (b) axial SPECT image, (c) axial SPECT/CT fusion image, (d) coronal maximal intensity projection (MIP) CT image, (e) coronal MIP SPECT image, and (f) coronal MIP SPECT/CT fusion image of a U-87 MG tumor-bearing mouse at 4 h postinjection of [^{67}Ga]**4**. Arrows indicate the site where U-87 MG cells were inoculated.

increasing the types of applicable radionuclides would be useful in the clinical because cancer diagnoses and therapy tailored to patients or/and hospitals can be performed. Radiotheranostics with multiradionuclides could contribute to developing personalized medicine and thus provide significant benefits to patients in the future.

■ ASSOCIATED CONTENT

Supporting Information

The Supporting Information is available free of charge at https://pubs.acs.org/doi/10.1021/acs.molpharmaceut.1c00460.

Biodistribution data of tracers in tumor-bearing mice (PDF)

■ AUTHOR INFORMATION

Corresponding Author

Kazuma Ogawa − *Institute for Frontier Science Initiative, Kanazawa University, Kanazawa 920-1192, Japan; Graduate School of Medical Sciences, Kanazawa University, Kanazawa 920-1192, Japan;* orcid.org/0000-0002-1691-7302; Phone: 81-76-234-4460; Email: kogawa@p.kanazawa-u.ac.jp; Fax: 81-76-234-4459

Authors

Hiroaki Echigo − *Graduate School of Medical Sciences, Kanazawa University, Kanazawa 920-1192, Japan*

Kenji Mishiro − *Institute for Frontier Science Initiative, Kanazawa University, Kanazawa 920-1192, Japan;* orcid.org/0000-0002-5071-7574

Saki Hirata − *Graduate School of Medical Sciences, Kanazawa University, Kanazawa 920-1192, Japan*

Kohshin Washiyama − *Advanced Clinical Research Center, Fukushima Global Medical Science Center, Fukushima Medical University, Fukushima 960-1295, Japan;* orcid.org/0000-0002-9908-8756

Yoji Kitamura − *Research Center for Experimental Modeling of Human Disease, Kanazawa University, Kanazawa, Ishikawa 920-8640, Japan*

Kazuhiro Takahashi − *Advanced Clinical Research Center, Fukushima Global Medical Science Center, Fukushima Medical University, Fukushima 960-1295, Japan*

Kazuhiro Shiba − *Research Center for Experimental Modeling of Human Disease, Kanazawa University, Kanazawa, Ishikawa 920-8640, Japan*

Seigo Kinuya − *Department of Nuclear Medicine, Kanazawa University Hospital, Kanazawa University, Kanazawa, Ishikawa 920-8641, Japan*

Complete contact information is available at: https://pubs.acs.org/10.1021/acs.molpharmaceut.1c00460

Notes

The authors declare no competing financial interest.

■ ACKNOWLEDGMENTS

This work was supported in part by Grants-in-Aid for Scientific Research (21H02867) from the Ministry of Education, Culture, Sports, Science and Technology, Japan, Mitani Foundation for Research and Development, Pancreas Research Foundation of Japan, Kanazawa University SAKIGAKE project 2020, and Program of the Network-type Joint Usage/Research Center for Radiation Disaster Medical Science.

■ REFERENCES

(1) Kelkar, S. S.; Reineke, T. M. Theranostics: combining imaging and therapy. *Bioconjugate Chem.* **2011**, *22*, 1879−903.

(2) Herrmann, K.; Schwaiger, M.; Lewis, J. S.; Solomon, S. B.; McNeil, B. J.; Baumann, M.; Gambhir, S. S.; Hricak, H.; Weissleder, R. Radiotheranostics: a roadmap for future development. *Lancet Oncol.* **2020**, *21*, e146−e156.

(3) Mishiro, K.; Hanaoka, H.; Yamaguchi, A.; Ogawa, K. Radiotheranostics with radiolanthanides: Design, development strategies, and medical applications. *Coord. Chem. Rev.* **2019**, *383*, 104−131.

(4) Ogawa, K. Development of Diagnostic and Therapeutic Probes with Controlled Pharmacokinetics for Use in Radiotheranostics. *Chem. Pharm. Bull.* **2019**, *67*, 897−903.

(5) Jadvar, H.; Chen, X.; Cai, W.; Mahmood, U. Radiotheranostics in Cancer Diagnosis and Management. *Radiology* **2018**, *286*, 388−400.

(6) Parker, C.; Lewington, V.; Shore, N.; Kratochwil, C.; Levy, M.; Linden, O.; Noordzij, W.; Park, J.; Saad, F. Targeted Alpha Therapy, an Emerging Class of Cancer Agents: A Review. *JAMA Oncol.* **2018**, *4*, 1765−1772.

(7) Nelson, B. J. B.; Andersson, J. D.; Wuest, F. Targeted Alpha Therapy: Progress in Radionuclide Production, Radiochemistry, and Applications. *Pharmaceutics* **2020**, *13*, No. 49.

(8) Kratochwil, C.; Bruchertseifer, F.; Giesel, F. L.; Weis, M.; Verburg, F. A.; Mottaghy, F.; Kopka, K.; Apostolidis, C.; Haberkorn, U.; Morgenstern, A. ^{225}Ac-PSMA-617 for PSMA-Targeted alpha-Radiation Therapy of Metastatic Castration-Resistant Prostate Cancer. *J. Nucl. Med.* **2016**, *57*, 1941−1944.

(9) Zalutsky, M. R.; Vaidyanathan, G. Astatine-211-labeled radiotherapeutics: an emerging approach to targeted alpha-particle radiotherapy. *Curr. Pharm. Des.* **2000**, *6*, 1433−55.

(10) Ogawa, K.; Takeda, T.; Mishiro, K.; Toyoshima, A.; Shiba, K.; Yoshimura, T.; Shinohara, A.; Kinuya, S.; Odani, A. Radiotheranostics Coupled between an At-211-Labeled RGD Peptide and the

Corresponding Radioiodine-Labeled RGD Peptide. *ACS Omega* **2019**, *4*, 4584−4591.
(11) Aoki, M.; Zhao, S.; Takahashi, K.; Washiyama, K.; Ukon, N.; Tan, C.; Shimoyama, S.; Nishijima, K. I.; Ogawa, K. Preliminary Evaluation of Astatine-211-Labeled Bombesin Derivatives for Targeted Alpha Therapy. *Chem. Pharm. Bull.* **2020**, *68*, 538−545.
(12) Byk, G.; Cohen-Ohana, M.; Raichman, D. Fast and versatile microwave-assisted intramolecular Heck reaction in peptide macrocyclization using microwave energy. *Biopolymers* **2006**, *84*, 274−82.
(13) Ogawa, K.; Yu, J.; Ishizaki, A.; Yokokawa, M.; Kitamura, M.; Kitamura, Y.; Shiba, K.; Odani, A. Radiogallium complex-conjugated bifunctional peptides for detecting primary cancer and bone metastases simultaneously. *Bioconjugate Chem.* **2015**, *26*, 1561−70.
(14) Ogawa, K.; Ishizaki, A.; Takai, K.; Kitamura, Y.; Kiwada, T.; Shiba, K.; Odani, A. Development of novel radiogallium-labeled bone imaging agents using oligo-aspartic acid peptides as carriers. *PLoS One* **2013**, *8*, No. e84335.
(15) Ogawa, K.; Takeda, T.; Yokokawa, M.; Yu, J.; Makino, A.; Kiyono, Y.; Shiba, K.; Kinuya, S.; Odani, A. Comparison of Radioiodine- or Radiobromine-Labeled RGD Peptides between Direct and Indirect Labeling Methods. *Chem. Pharm. Bull.* **2018**, *66*, 651−659.
(16) Mizuno, Y.; Uehara, T.; Hanaoka, H.; Endo, Y.; Jen, C. W.; Arano, Y. Purification-Free Method for Preparing Technetium-99m-Labeled Multivalent Probes for Enhanced in Vivo Imaging of Saturable Systems. *J. Med. Chem.* **2016**, *59*, 3331−9.
(17) Effendi, N.; Mishiro, K.; Shiba, K.; Kinuya, S.; Ogawa, K. Development of Radiogallium-Labeled Peptides for Platelet-Derived Growth Factor Receptor beta (PDGFRbeta) Imaging: Influence of Different Linkers. *Molecules* **2020**, *26*, 41.
(18) Di Cosmo, C.; Liao, X. H.; Dumitrescu, A. M.; Philp, N. J.; Weiss, R. E.; Refetoff, S. Mice deficient in MCT8 reveal a mechanism regulating thyroid hormone secretion. *J. Clin. Invest.* **2010**, *120*, 3377−88.
(19) Ogawa, K.; Mizuno, Y.; Washiyama, K.; Shiba, K.; Takahashi, N.; Kozaka, T.; Watanabe, S.; Shinohara, A.; Odani, A. Preparation and evaluation of an astatine-211-labeled sigma receptor ligand for alpha radionuclide therapy. *Nucl. Med. Biol.* **2015**, *42*, 875−9.
(20) Ogawa, K.; Mukai, T.; Inoue, Y.; Ono, M.; Saji, H. Development of a novel ^{99m}Tc-chelate-conjugated bisphosphonate with high affinity for bone as a bone scintigraphic agent. *J. Nucl. Med.* **2006**, *47*, 2042−7.
(21) Chen, X.; Hou, Y.; Tohme, M.; Park, R.; Khankaldyyan, V.; Gonzales-Gomez, I.; Bading, J. R.; Laug, W. E.; Conti, P. S. Pegylated Arg-Gly-Asp peptide: ^{64}Cu labeling and PET imaging of brain tumor $\alpha_v\beta_3$-integrin expression. *J. Nucl. Med.* **2004**, *45*, 1776−83.
(22) Hayes, R. L. The medical use of gallium radionuclides: a brief history with some comments. *Semin. Nucl. Med.* **1978**, *8*, 183−91.
(23) Teze, D.; Sergentu, D. C.; Kalichuk, V.; Barbet, J.; Deniaud, D.; Galland, N.; Maurice, R.; Montavon, G. Targeted radionuclide therapy with astatine-211: Oxidative dehalogenation of astatobenzoate conjugates. *Sci. Rep.* **2017**, *7*, No. 2579.
(24) Meyer, G.-J. Astatine. *J. Labelled Compd. Radiopharm.* **2018**, *61*, 154−164.
(25) Lindegren, S.; Albertsson, P.; Back, T.; Jensen, H.; Palm, S.; Aneheim, E. Realizing Clinical Trials with Astatine-211: The Chemistry Infrastructure. *Cancer Biother. Radiopharm.* **2020**, *35*, 425−436.
(26) Larsen, R. H.; Slade, S.; Zalutsky, M. R. Blocking [^{211}At]-astatide accumulation in normal tissues: preliminary evaluation of seven potential compounds. *Nucl. Med. Biol.* **1998**, *25*, 351−7.
(27) Yoshimoto, M.; Ogawa, K.; Washiyama, K.; Shikano, N.; Mori, H.; Amano, R.; Kawai, K. $\alpha_v\beta_3$ Integrin-targeting radionuclide therapy and imaging with monomeric RGD peptide. *Int. J. Cancer* **2008**, *123*, 709−15.
(28) Janssen, M. L.; Oyen, W. J.; Dijkgraaf, I.; Massuger, L. F.; Frielink, C.; Edwards, D. S.; Rajopadhye, M.; Boonstra, H.; Corstens, F. H.; Boerman, O. C. Tumor targeting with radiolabeled $\alpha_v\beta_3$ integrin binding peptides in a nude mouse model. *Cancer Res.* **2002**, *62*, 6146−51.
(29) Singh, B.; Fu, C.; Bhattacharya, J. Vascular expression of the $\alpha_v\beta_3$-integrin in lung and other organs. *Am. J. Physiol.: Lung Cell. Mol. Physiol.* **2000**, *278*, L217−26.

https://doi.org/10.1021/acs.molpharmaceut.1c00460
Mol. Pharmaceutics XXXX, XXX, XXX−XXX